Spatiotemporal characteristics of the collisionless rf sheath and the ion energy distributions arriving at rf-biased electrodes

Zhong-Ling Dai,* You-Nian Wang, and Teng-Cai Ma
Department of Physics, Dalian University of Technology, Dalian 116023, People's Republic of China
(Received 2 August 2001; revised manuscript received 26 November 2001; published 13 February 2002)

A self-consistent fluid model is proposed for describing collisionless radio-frequency (rf) sheaths driven by a sinusoidal current source. This model includes all time-dependent terms in ion fluid equations, which are commonly ignored in some analytical models and numerical simulations. Moreover, an equivalent circuit model is introduced to determine self-consistently the relationship between the instantaneous potential at a rf-biased electrode and the sheath thickness. The time-dependent voltage wave form, the sheath thickness and the ion flux at the electrode as well as the spatiotemporal variations of the potential, the electric field and the ion density inside the sheath are calculated for various rf powers and ratios of the rf frequency to the ion plasma frequency. The ion energy distributions (IEDs) impinging on the rf-biased electrode are also calculated with the ion flux at the electrode. The numerical results show that the frequency ratio is a crucial parameter determining the spatiotemporal variations of the rf sheath and the shape of the IEDs.

DOI: 10.1103/PhysRevE.65.036403 PACS number(s): 52.65.−y, 52.40.Hf

I. INTRODUCTION

Radio-frequency (rf) gas discharges currently play a major role in the microelectronics industry for fabrication of the new generation ultra-large-scale integrated circuits. These discharges are typically used for stripping of photoresist, depositing of organic and inorganic thin films, and anisotropic etching of semiconductor, oxide, and metal surfaces. In processing plasmas, the ion energy and ion angular distributions (IEDs and IADs) arriving at substrates are crucial in determining ion anisotropy and etch rates. The electrode a substrate is placed upon is often independently rf biased in order to control the ion impact energy, causing a rf sheath adjacent to the substrate electrode. In order to accurately predict the IEDs and IADs, it is important to determine exact details of the spatiotemporal variations of the electric field within the rf sheath and the time dependence of the sheath thickness.

Over the past decades, the behavior of the rf sheath has been a topic of much scientific interest due to its importance. Based on the ion hydrodynamics coupled to the Poisson's equation, various sheath models [1–13] have been developed to describe the characteristics of the rf sheath. In general, it is difficult to get analytical solutions for the sheath due to its strongly nonlinear processes. A crucial parameter for simplifying the sheath dynamics is the ratio of the rf frequency to the ion plasma frequency $\beta=\omega/\omega_{pi}$. When the rf frequency is much smaller than the ion plasma frequency ($\beta\ll 1$), the ions respond to the instantaneous sheath potential and cross the sheath in a small fraction of a rf cycle. A quasistatic model [1] has been adopted to describe the nonlinear processes in the low-frequency range. In this model, sheath properties at different times in a rf cycle are the same as those of a direct current (dc) with a potential equal to the instantaneous value.

In the high-frequency range ($\beta\gg 1$), the ions take many rf cycles to cross the sheath and can no longer respond to the instantaneous sheath potential. Instead, the ion dynamics is governed by a time-averaged field in the sheath. A simplified model has been proposed by Lieberman to describe the collisionless [2], and the collisional sheath [3]. This model ignores all time-dependent terms in the ion fluid equations and uses a step model in which the electron density drops abruptly to zero at the electron sheath boundary. With the simplified model, analytical expressions have been obtained for various sheath parameters such as the dc sheath voltage, the sheath capacitance, and the stochastic heating power. However, Refs. [2] and [3] completely neglect the ion and electron currents in the rf sheath, which is adequate only to the extremely high rf sheath voltage. Based on the step model, other authors [4–6] studied the characteristics of the rf sheath by taking into account the electron and ion conduction currents in the sheath. Making use of suitable boundary conditions, Gierling and Riemann [7] introduced a consistent step model. Beyond the step model, Riemann [8] gave an improved description of the rf sheath by taking correctly into account the distribution function of ions entering the rf sheath. Recently, Edelberg and Aydil [9] refined further the dynamic model of the rf sheath by coupling an equivalent circuit model to the ion fluid equations, which is used for predicting consistently the time-dependent potential on the electrode.

In the intermediate frequency range ($\beta\sim 1$), it is difficult to obtain an analytical representation of the sheath because the ion inertia allows it to only partially respond to the time-varying fields in the sheath. Miller and Riley [10] introduced a ''damped potential'' to model the ion dynamics in this frequency range, which assumes that the ions respond to the damped potential. Panagopoulos and Economou [11] extended the damped potential model and calculated the IEDs for a collisionless sheath. Taking into account all time-dependent terms in the ion fluid equations, Bose *et al.* [12] found that the ion flux indeed oscillates significantly in a rf cycle for values of $\beta\sim 1$. For simplifying numerical calculations, however, Bose *et al.* assumed that a sinusoidal voltage $V_1[\sin(\omega t)+1]$ is applied on the electrode and the amplitude V_1 is a given parameter. It is well known [2] that although a

*Email address: daizhl@dlut.edu.cn

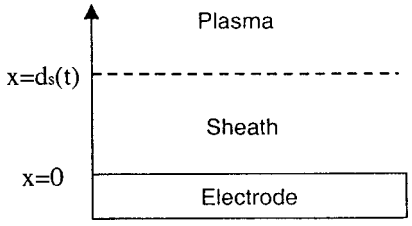

FIG. 1. Schematic diagram of the rf sheath model, electrode located at $x=0$ and the plasma-sheath boundary located at $x=d_s(t)$.

sinusoidal rf current source is applied on the electrode, the voltage on the electrode is not exactly sinusoidal due to the effects of the sheath loading. In fact, both the forms and amplitudes of the voltage on the electrode are unknown and should be determined consistently by the current balance condition on the electrode, just as the equivalent circuit model [9]. Most recently, Sobolewski [13] presented a rf sheath model that does fully account for the time-dependent ion motion for β values from 0.006 to 1.8. It should be stressed that the step model about the electron density in the sheath is also adopted in Sobolewski's work to simplify the solution of Poisson's equation in the sheath.

In this paper, we wish to present a self-consistent dynamic model of collisionless rf sheaths that includes all time-dependent terms in the ion fluid equations and is coupled to the equivalent circuit model. Further, we try to investigate the IEDs on the electrode with the calculated ion flux. This article is outlined as follows. In Sec. II the basic model is described, including the ion fluid equations, the equivalent circuit model, and the boundary conditions. Then, in Sec. III, we present some numerical solutions of the sheath model and show the time-dependent voltage wave form, sheath thickness, and ion flux, as well as the spatiotemporal variation of potential, electric field, and ion density for various rf-bias frequencies or various rf-bias power values. Using the calculated ion flux, the ion energy distribution bombarding a rf-biased electrode is determined numerically in Sec. IV. Finally, a short summary is given in Sec. V.

II. MODEL DESCRIPTION

We consider that a rf-bias power is applied to an electrode inside a low-pressure plasma. Then, a rf sheath will be formed near the electrode surface, as shown in Fig. 1. The one-dimensional configuration, with the electrode placed at $x=0$, is adopted. Under the low-pressure condition, due to the sheath thickness being much less than the mean free path of ions and neutral particles, it is reasonable to neglect collisions between ions and neutral particles. Also, we can neglect the ion thermal motion effects since the ion temperature is much smaller than the directional kinetic energy in the sheath regions. Thus, the one-dimensional spatiotemporal variation of the ion density, $n_i(x,t)$, the ion drift velocity, $u_i(x,t)$, and the electric potential inside the sheath, $V(x,t)$, are described by the cold ion fluid equations,

$$\frac{\partial n_i}{\partial t}+\frac{\partial (n_i u_i)}{\partial x}=0, \tag{1}$$

$$\frac{\partial u_i}{\partial t}+u_i\frac{du_i}{dx}=-\frac{e}{m_i}\frac{\partial V}{\partial x}, \tag{2}$$

and the Poisson equation,

$$\frac{\partial^2 V}{\partial x^2}=-\frac{e}{\varepsilon_0}(n_i-n_e), \tag{3}$$

where m_i is ion mass, e is the electronic charge, ε_0 is the permitivity of free space, and $n_e(x,t)$ is the electron density. In previous sheath model [2–9], the time-derivative terms in Eqs. (1) and (2) are omitted and the potential $V(x,t)$ in Eq. (2) is replaced by a time-averaged potential, which is valid in the high-frequency limits $\beta \gg 1$. In the present model, we retain all time-dependent terms in the ion fluid equations, so that the model is valid over a wide frequency range, from $\beta \ll 1$ to $\beta \gg 1$.

Due to the electron plasma frequency ω_{pe} being much higher than the rf frequency ω, we can assume that the electrons are inertialess and respond to the instantaneous electric field. In contrast to the step model [2–6], here we consider that the electron density in the sheath changes continuously and is given by the Boltzmann distribution,

$$n_e(x,t)=n_0\exp\left(\frac{eV(x,t)}{k_B T_e}\right), \tag{4}$$

where n_0 is the plasma density, T_e is the electron temperature, and k_B is the Boltzmann constant.

To solve Eqs. (1)–(3), the appropriate boundary conditions at the plasma-sheath interface must be chosen. Compared to the dc sheath, the rf sheath boundary conditions are quite complex and the boundary may oscillate in a rf cycle. However, Riemann [14] pointed out that Bohm criterion is still valid for rf sheaths. Thus, we assume that at the plasma-sheath boundary $x=d_s(t)$ the ion density should be equal to the electron density, i.e., the quasineutral condition,

$$n_i(d_s,t)=n_e(d_s,t). \tag{5}$$

Besides, we also assume that ions enter the sheath with a velocity equal to the Bohm velocity $u_B=\sqrt{k_B T_e/m_i}$, i.e.,

$$u_i(d_s,t)=u_B. \tag{6}$$

Finally, we assume that the potential at the sheath edge is approximately zero, i.e.,

$$V(d_s,t)=0, \tag{7}$$

and take the value of the potential at the electrode ($x=0$) to be

$$V(0,t)=V_e(t), \tag{8}$$

where $V_e(t)$ will be obtained by coupling Eqs. (1)–(3) to a current balance equation, see the following content.

Among the above boundary conditions, unfortunately, $V_e(t)$ is unknown. For simplifying numerical analysis, Bose *et al.* [12] proposed a sinusoidal voltage $V_e(t)=V_1[\sin(\omega t)$

+1]. As a matter of fact, the instantaneous voltage depends on not only the applied rf power, but also instantaneous characteristics of the sheath itself. An equivalent circuit model has been introduced by Edelberg and Aydil [9] to determine self-consistently the relationship between the instantaneous voltage $V_e(t)$ and the instantaneous sheath thickness $d_s(t)$. In the model, the sheath is modeled as a parallel combination of a diode, a capacitor, and a current source. The current through the diode represents the variation of the electron current as a function of the voltage at the electrode,

$$I_e(t)=\frac{eu_e n_0 A}{4}\exp\left(\frac{eV_e(t)}{k_B T_e}\right), \tag{9}$$

where A is the electrode area and $u_e=\sqrt{8k_B T_e/\pi m_e}$ is the mean velocity of an electron with mass m_e. The current source represents the current due to ions incidence onto the electrode, which is expressed by

$$I_i(t)=eu_i(0,t)n_i(0,t)A. \tag{10}$$

The current through the capacitor results from the time variation of charge at electrode and can be derived as

$$I_d(t)=\frac{dQ}{dt}=\frac{d(C_s V_e)}{dt}=C_s\frac{dV_e}{dt}+V_e\frac{dC_s}{dt}, \tag{11}$$

where $C_s(t)=\varepsilon_0 A/d_s(t)$ is the time-dependent sheath capacitance. Assuming that the rf current applied at the electrode is sinusoidal, we can obtain the current balance equation,

$$I_i(t)-I_e(t)-C_s(t)\frac{dV_e(t)}{dt}-V_e(t)\frac{dC_s(t)}{dt}=I_{\max}\sin(\omega t), \tag{12}$$

where $I_{\max}$ is the amplitude of applied rf-bias current. It should be stressed that this current balance equation is also obtained by Edelberg and Aydil [9], but they assumed a constant ion current $eu_B n_0 A$ at electrode, and neglected the second term $V_e dC_s/dt$ on the right side of Eq. (11). In contrast, considering that the ion dynamics is governed by the instantaneous electric field, we adopt a time-dependent ion current $I_i(t)$ at the electrode. Moreover, the second term $V_e dC_s/dt$ is retained in this paper in order to make the model fully consistent.

Now we get a set of closed nonlinear equations that determines the spatiotemporal dependence of the rf sheath. The above equations with the boundary conditions will be solved numerically in Sec. III by using a finite difference scheme with an iterative process.

III. NUMERICAL RESULTS OF THE rf SHEATH

In this section we use numerical techniques to solve the fluid equations and the current balance equation with boundary conditions. By solving the current balance equation (12) with the fourth-order Runge-Kutta method, we can first obtain the potential drop across the sheath, i.e., the voltage $V_e(t)$ of the electrode. The initial guesses of the instantaneous sheath thickness $d_s(t)$, the ion density at the electrode $n_i(0,t)$, and the ion velocity at the electrode $u_i(0,t)$ are all chosen as uniform values. With the obtained voltage $V_e(t)$, we then solve the fluid equations and the Poisson's equation [Eqs. (1)–(3)] using a second-order finite difference scheme in space and an explicit scheme in time, which will yield new $d_s(t)$, $n_i(0,t)$, and $u_i(0,t)$. The iteration is repeated until the solutions converge to a self-consistent periodic steady state. In the following simulations, we take an argon discharge as an example in which all the base values of the input parameters, such as $n_0=2.1\times10^{11}$ cm^{-3}, $k_B T_e=3$ eV, and $A=325$ cm^2 (the electrode area), come from the actual experiments [9]. The rf-bias power is calculated from the time-dependent voltage and current wave forms as follows:

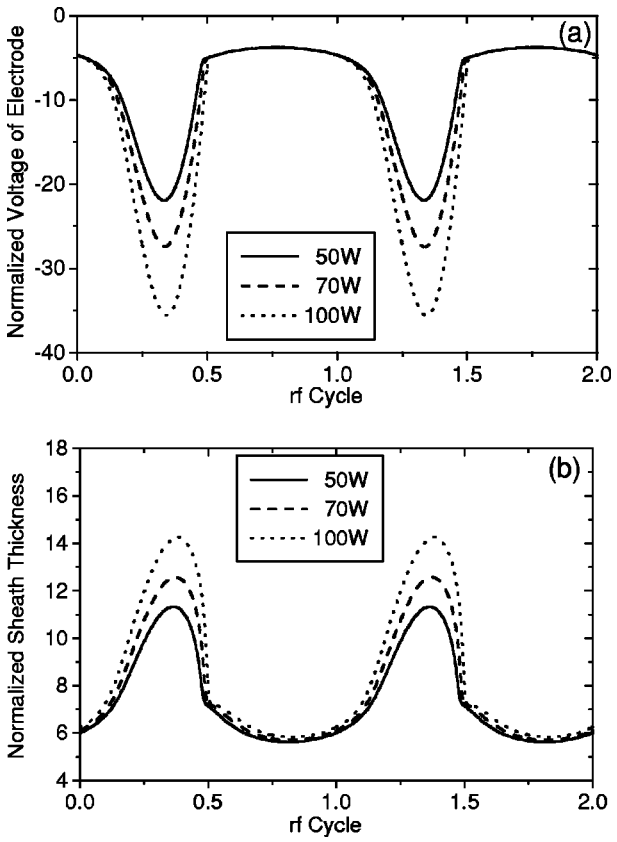

FIG. 2. The effect of rf-bias power on (a) the instantaneous electrode voltage $V_e(t)$ for an Ar plasma and (b) the time-dependent electron sheath thickness $d_s(t)$. The frequency ratio β is 0.25.

$$P=\frac{1}{\tau}\int_0^{\tau} V_e(t)I(t)dt, \tag{13}$$

where $\tau=2\pi/\omega$ is the rf cycle and $I(t)=I_{\max}\sin(\omega t)$. Furthermore, for convenience in calculations, we use the Debye length λ_d, the ion plasma frequency ω_{pi}, the Bohm velocity u_B, the plasma density n_0, and the electron temperature $k_B T_e/e$ to nondimensionalize the position x, the time t, the ion velocity u_i, the ion density n_i, and the potential V, respectively.

Figure 2 displays (a) the time dependence of the voltage

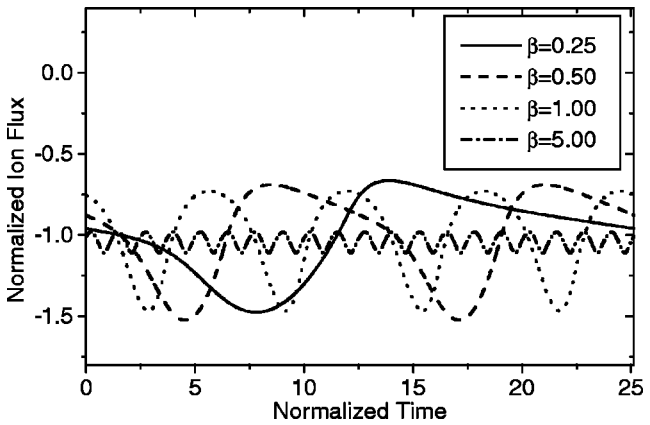

FIG. 3. The time-dependent ion flux $n_i u_i$ incident onto the rf-biased electrode for different values of the frequency ratio β. The rf-bias power is 50 W.

of the electrode and (b) the sheath thickness for different rf-bias power values and a given rf-bias frequency ratio $\beta = 0.25$. It is clear that for any time in the rf cycle the amplitude of the voltage of electrode and the sheath thickness increases with increasing rf-bias power. One can also observe that as the potential wave form reaches its maximum voltage drop, the sheath thickness reaches its maximum.

The time dependence of the ion flux impinging on the electrode is shown in Fig. 3 for different values of the frequency ratio β. When the rf-bias frequency is less than the ion plasma frequency, i.e., $\beta \leqslant 1$, the ion flux oscillates strongly and its amplitudes deviate from the constant ion flux $n_0 u_B$ significantly, which has been reported only in a few literatures [12,13]. At high rf-bias frequency limits such as $\beta = 5$, the amplitude of the ion flux is very small and almost closes to the constant ion flux $n_0 u_B$. This shows that it is reasonable to assume a constant ion flux through the sheath only in the high-frequency ratio limits, which results from that the ions respond to the time-averaged electric field instead of instantaneous sheath electric field in this case.

We should stress that the previous works [1–11] are valid only for high-frequency ratio β due to neglecting the time-dependent terms in the ion fluid equations. In the present paper, however, all the time-dependent term in the fluid equations are retained, so the present model may describe the ion dynamics in the sheath for arbitrary frequency ratio β. To illustrate clearly this difference, Figs. 4(a) and 4(b) show the maximum sheath voltage drop $V_{\max}$ and the maximum sheath thickness $d_{\max}$ for a wide range of β from 0.1 to 10, respectively. It can been seen that in the low and intermediate frequency ratio ($\beta \ll 1$ and $\beta \sim 1$), the results predicted by Edelberg-Aydil model [9] deviate significantely from that in our simulation. However, both of the results approach each other in the high-frequency range ($\beta \gg 1$). For comparing our results with Edelberg-Aydil's results, in Figs. 4(a) and 4(b) we have neglected contributions coming from the term $V_e dC_s/dt$ on the right side of Eq. (11) since this term is also neglected in Edelberg-Aydil's work.

We also plot the spatiotemporal variations of the ion density, the potential, and the electric field inside the sheath in [Figs. 5(a)–5(c)] for a given rf-bias power $P = 50$ W and a

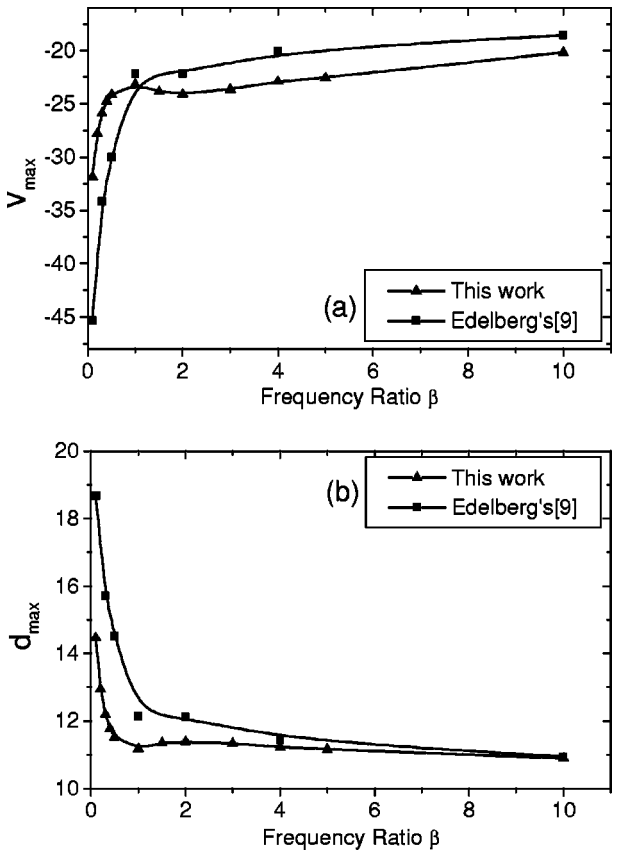

FIG. 4. The maximum sheath voltage drop $V_{\max}$ and the maximum sheath thickness $d_{\max}$ for a wide range of β. The ion density and the rf-bias power are fixed at 3.0×10^{11} cm^{-3} and 100 W, respectively.

given frequency ratio $\beta = 0.25$, respectively. We notice from Fig. 5(a) that the ion density changes obviously with the spatial variable, but does gently with the time. Figures 5(b) and 5(c) illustrate that the spatial variations of the potential and the electric field vary significantly near the electrode and the temporal profiles of them oscillate periodically with the time.

IV. ION ENERGY DISTRIBUTIONS

It has been seen from the results shown in Sec. III that the ion dynamics in the rf sheath is modulated by the sheath electric field. One may expect that the modulation of the rf sheath electric field will affect the energy distributions of ions impinging on the electrode (or the substrate) surface. During the past decades, many researchers have calculated IEDs with different rf sheath models. In the high-frequency regime for a collisionless rf sheath, Benoit-Cattin and Bernard [15] obtained an analytical expression of the IED by assuming a sinusoidal sheath electric field with a constant sheath width. Metze *et al.* [16] calculated the potential wave forms across a collisionless sheath through an equivalent circuit model and determined the IEDs by solving the ion motion equation in the rf sheath. Assuming a parametric model for the spatially linear and time-dependent electric field within the rf sheath, Kushner calculated the IEDs and the

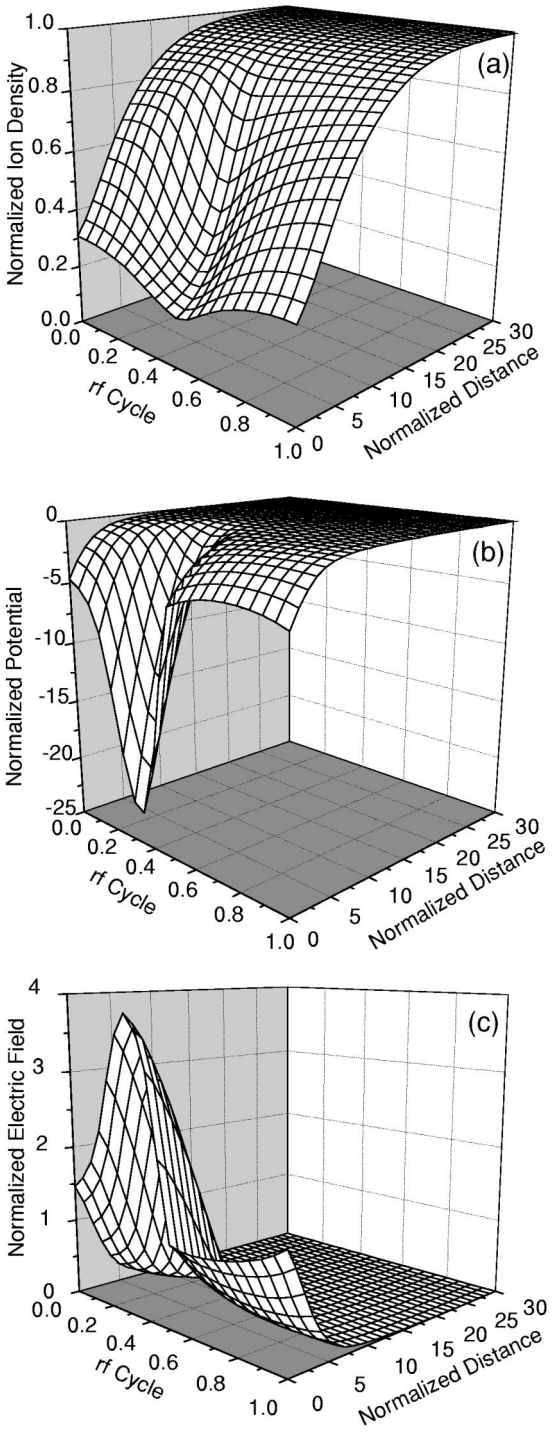

FIG. 5. The spatiotemporal variation of (a) the ion density $n_i(x,t)$, (b) the potential $V(x,t)$, and (c) the electric field $E(x,t)$ inside the sheath during one rf cycle. The rf-bias power and the frequency ratio are 50 W and 0.25, respectively.

IADs using the Monte Carlo model for ion trajectories [17]. Edelberg and Aydil [9] also simulated the IEDs in a collisionless rf sheath using the Monte Carlo method in conjunction with their sheath model in which the ion dynamics is determined by a time-averaged sheath electric field. More recently, giving an average potential profile and its time dependence, Misakian and Wang [18] also calculated the shape

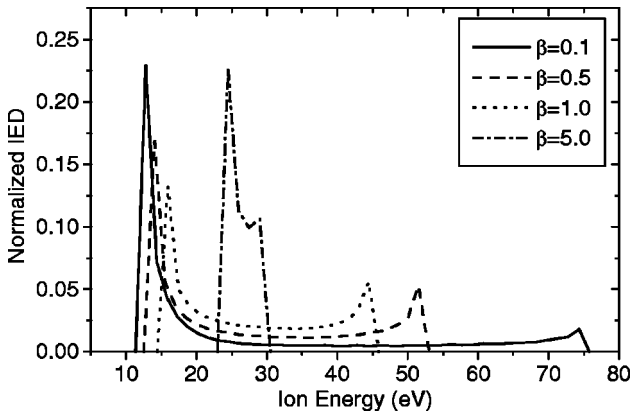

FIG. 6. Effects of the frequency ratio β on the ion energy distributions for a given rf-bias power $P=50$ W.

of IEDs using the Monte Carlo method. In a review article [19], Kawamura *et al.* made a detailed analysis of the IEDs about the rf sheath.

In this section, we can calculate directly the IEDs with the ion flux impinging on the rf-bias electrode. It should be stressed that this method to calculate the IEDs is suitable only for collisionless sheaths. We know from the Sec. III that both the ion flux $J_i=n_iu_i$ and the ion energy $E=m_iu_i^2/2$ on the electrode at any time in one rf cycle can be obtained with the self-consistent fluid model of the sheath. Consequently, one can further obtain the number N of ions arriving at the electrode in one rf cycle with energy below a certain value. Thus, the IEDs can be expressed by

$$f(E)=\frac{dN(E)}{dE}. \tag{14}$$

In the following calculations for IEDs, we still take the argon discharge as an example, and the plasma parameter and the electrode area are the same as what are used in Sec. III. Figure 6 shows the frequency ratio β dependence of the ion energy distributions for the argon plasma with a given rf-bias power $P=50$ W. Within considered frequency ratio ranges, the IEDs have bimodal shapes that have been expected by other theoretical models [9,15,17] and observed by experiments [9,20–22]. In the low-frequency limits ($\beta \ll 1$), ions cross the sheath in a small fraction of one rf cycle and respond to the instantaneous sheath voltage. Thus, their final energies depend strongly on the phase of the rf cycle in which they enter the sheath and the two peaks in the IEDs correspond to the minimum and maximum sheath potential drops. Ions traversing the sheath during the period in the rf cycle where the potential drop across the sheath is small will arrive at the electrode with low energies and contribute to the low-energy peak in the IED. In contrast, the ions entering and traversing the sheath during the period in the rf cycle where the potential drop across the sheath is large will arrive at the electrode with high energies and contribute to the high-energy peak in the IED. For the high-frequency limits ($\beta \gg 1$), however, the ions take many rf cycles to cross the sheath and can no longer respond to the instantaneous sheath electric field. Instead, the ions respond only to a time-

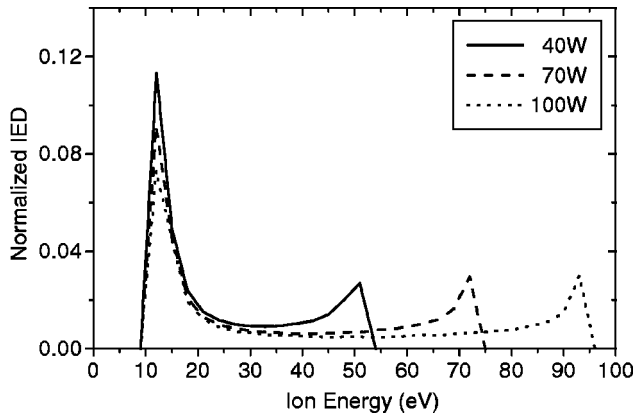

FIG. 7. Effects of the rf-bias power on the ion energy distributions for a given the frequency raito $\beta=0.25$.

averaged electric field in the sheath and the phase of the cycle in which they enter the sheath becomes unimportant, resulting in a narrower IED. As β value increases, the IED width shrinks and the two peaks of the IED approach each other.

In Fig. 7 we also show the effects of the rf-bias power on the IEDs for a given frequency ratio $\beta=0.25$. We notice that as the rf-bias power is increased, the locations of the high-energy peaks shift towards the high-energy regime and increase linearly as a function of the rf-bias power approximately, while the locations of low-energy peaks does not move. And also, with the increasing rf-bias power, the height of the low-energy peak drops, but the height of the high-energy peak does not change significantly.

Finally, in Fig. 8 we compare our numerical results of IED with experimentally measured IED in an Ar plasma. The values of the input parameters in the simulation are identical with the measured in the experiment [9], i.e., rf-bias power $P=400$ W, rf-bias frequency $f=4$ MHz ($\beta=0.25$), plasma density $n_0=2.1\times10^{11}$ cm^{-3}, and the other base values are the same as those used in Sec. III. In the figure we also show the simulation results of Edelberg and Aydil [9]. One can observe that our numerical results accurately predict the measured peak positions. Edelberg and Aydil also tried to compare their numerical results with experimental data, but for getting a comparable figure they had to adjust the power to 392 W and the plasma density to 3.5×10^{11} cm^{-3} in their simulations.

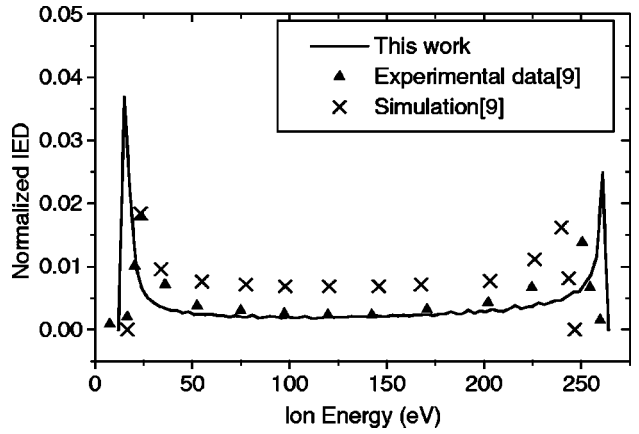

FIG. 8. Comparison of numerical results with experimental data [9] for IEDs in an Ar plasma for the rf-bias frequency 4 MHz ($\beta=0.25$). In our simulations and the expriment: the rf-bias power $P=400$ W and the plasma density $n_0=2.1\times10^{11}$ cm^{-3}; in the simulations [9], $P=392$ W and $n_0=3.5\times10^{11}$ cm^{-3}.

V. CONCLUSIONS

A self-consistent fluid model of a collisionless rf modulated sheath has been developed for studying the spatiotemporal characteristics of the sheath and predicting the energy distributions of ions impinging on a rf-biased electrode. The model includes all time-dependent terms in the ion fluid equations, which is valid for arbitrary frequency ratio β. Moreover, the instantaneous relationship between the voltage on the rf-biased electrode and the sheath thickness is determined by an equivalent circuit model with a time-dependent ion current on the electrode, which differs from the circuit model used in the simulations of Edelberg and Aydil [9] assuming a constant ion current on the electrode. It has been shown from the numerical results that in the low-rf-frequency regime ($\beta\leqslant1$) the ion flux on the electrode oscillates strongly with the time and its amplitude drops gradually with the increasing frequency ratio β, while the ion flux approaches the constant flux n_0u_B at the high-frequency limits ($\beta\gg1$). We have further found that the instantaneous variations of the sheath thickness and the voltage wave form on the electrode are almost synchronous, the spatiotemporal variations of the potential and the electric field within the sheath are very significant in the vicinity of the electrode, and the spatial drop of the ion density in the sheath is monotonous. Finally, with obtained ion flux, we have calculated the IEDs on the electrode and found that the IEDs has a bimodal shape and the width of the IED shrinks and the two peaks of the IED approach each other with the increasing rf frequency. Besides, the locations and heights of the two peaks in the IED are also affected by the rf-bias power. In conclusion, the frequency ratio $\beta=\omega/\omega_{pi}$ is a crucial parameter for determining the sheath characteristics, the sheath voltage wave form, and the shape of the IEDs.

The model proposed here does not take into account the collisions of ions with neutral particles in the sheath and is suitable only for describing sheaths in the low-pressure discharges, generally for the pressure lower than 10 mTorr. Nevertheless, in some processing plasmas, the discharge pressure can reach tens of milliTorr and collisional effects become important. In the future, we will extend the present paper to include both elastic and exchange collisions occurring in the rf sheath and simulate the IEDs and IADs on the electrode with the Monte Carlo method.

ACKNOWLEDGMENTS

This work was jointly supported by the National Natural Science Foundation of China (Grant Nos. 19975008 and 19835030) and the Grant for Striding-Century Excellent Scholar of the Ministry of Education State of China.

[1] A. Metze, D.W. Ernie, and H.J. Oskam, J. Appl. Phys. **60**, 3081 (1986).
[2] M.A. Lieberman, IEEE Trans. Plasma Sci. **16**, 638 (1988).
[3] M.A. Lieberman, IEEE Trans. Plasma Sci. **17**, 338 (1989).
[4] V.A. Godyak and N. Sternberg, Phys. Rev. A **42**, 2299 (1990).
[5] N. Sternberg and V.A. Godyak, J. Comput. Phys. **111**, 347 (1994).
[6] M.A. Sobolewski, Phys. Rev. E **56**, 1001 (1997).
[7] J. Gierling and K.U. Riemann, J. Appl. Phys. **83**, 3521 (1998).
[8] K.U. Riemann, J. Appl. Phys. **65**, 999 (1989).
[9] E.A. Edelberg and E.S. Aydil, J. Appl. Phys. **86**, 4799 (1999).
[10] P.A. Miller and M.E. Riley, J. Appl. Phys. **82**, 3689 (1997).
[11] T. Panagopoulos and D.J. Economou, J. Appl. Phys. **85**, 3435 (1999).
[12] D. Bose, T.R. Govindan, and M. Meyyappan, J. Appl. Phys. **87**, 7176 (2000).
[13] M.A. Sobolewski, Phys. Rev. E **62**, 8540 (2000).
[14] K.U. Riemann, Phys. Fluids B **4**, 2693 (1992).
[15] P. Benoit-Cattin and L.C. Bernard, J. Appl. Phys. **39**, 5723 (1968).
[16] A. Metze, D.W. Ernie, and H.J. Oskam, J. Appl. Phys. **65**, 993 (1989).
[17] M.J. Kushner, J. Appl. Phys. **58**, 4024 (1985).
[18] M. Misakian and Y. Wang, J. Appl. Phys. **87**, 3646 (2000).
[19] E. Kawamura, V. Vahedi, M.A. Lieberman, and C.K. Birdsall, Plasma Sources Sci. Technol. **8**, R45 (1999).
[20] K. Kohler, D.E. Horne, and J.W. Coburn, J. Appl. Phys. **58**, 3350 (1985).
[21] A.D. Kuypers and H.J. Hopman, J. Appl. Phys. **63**, 1894 (1988).
[22] C. Charles *et al.*, Phys. Plasmas **7**, 5232 (2000).